

# Formation energies of silicon self-interstitials using periodic coupled cluster theory

Faruk Salihbegović, Alejandro Gallo, and Andreas Grüneis

*Institute for Theoretical Physics, Vienna University of Technology (TU Wien). A-1040 Vienna, Austria, EU.*

(Dated: June 23, 2023)

We present a study of the self-interstitial point defect formation energies in silicon using a range of quantum chemical theories including the coupled cluster (CC) method within a periodic supercell approach. We study the formation energies of the X, T, H and C3V self-interstitials and the vacancy V. Our results are compared to findings obtained using different ab initio methods published in the literature and partly to experimental data. In order to achieve computational results that are converged with respect to system size and basis set, we employ the recently proposed finite size error corrections and basis set incompleteness error corrections. Our CCSD(T) calculations yield an order of stability of the X, H and T self-interstitials, which agrees both with quantum Monte Carlo results and with predictions obtained using the random-phase approximation as well as using screened hybrid functionals. Compared to quantum Monte Carlo results with backflow corrections, the CCSD(T) formation energies of X and H are only slightly larger by about 100 meV. However, in the case of the T self-interstitial, we find significant disagreement with all other theoretical predictions. Compared to quantum Monte Carlo calculations, CCSD(T) overestimates the formation energy of the T self-interstitial by 1.2 eV. Although this can partly be attributed to strong correlation effects, more accurate electronic structure theories are needed to understand these findings.

## I. INTRODUCTION

After more than 60 years of sophisticated silicon device production, one might think that all the details of this material are fully understood, especially knowing that the manufacturing of today's nanometer-sized transistors requires near-atomic accuracy. However, as a direct result of this miniaturization, the accidental creation of a single trapping center can be large enough to alter the electronic properties of the sample, making this issue the most feared phenomenon in the industry [1].

To better understand the influence of single isolated vacancies and interstitials, these have to be produced experimentally. This can be achieved with 1–3 MeV electron irradiation performed at cryogenic temperatures. The identification of these centers is possible through characterization techniques like electron paramagnetic spectroscopy (EPR), which is capable of targeting the atomic distortion triggered by the form of the localized electronic density [2, 3]. Infrared optical absorption and deep-level transient spectroscopy can also be used to identify center-induced states within the semiconductor gap [4–6]. The availability of experimental data motivated the development of simple theoretical models geared towards quantitatively reproducing the basic features of these defects. Furthermore, the rapid growth in computational resources made it possible to perform ab initio calculations to model and understand their properties thoroughly on an atomistic level.

Point defects, such as vacancies, interstitials and anti-site defects, are the only thermodynamically stable defects at finite temperatures [7]. The presence of point defects often controls the kinetics of the material and can therefore fundamentally alter its electronic, optical and mechanical properties. This makes the understanding of point defects technologically important for a wide range of applications such as doping of semiconductors [8–11],

production of quantum devices [12, 13], and controlling the transition temperature of shape memory alloys [14].

Of all materials, silicon is one of the most important for industrial use and plays a crucial role in a wide variety of devices, e.g., advanced electronic devices, power devices, solar cells, and microelectronic systems. In all these applications, Czochralski (CZ) and floating zone (FZ) silicon single crystals are used (except for some solar cells) [15]. The diffusion characteristics and thermodynamics of silicon self-interstitials and vacancies dominate the doping and annealing processes for electronics applications [9, 10]. However, the understanding of self-diffusion in silicon remains incomplete despite decades of research [12, 16–36]. Questions regarding the role of the self-interstitials and the vacancy in the self-diffusion remain. One of the remaining questions, which needs to be addressed using quantum mechanical methods, is the formation energy of the silicon self-interstitials and vacancy. The most widely used method in this regard is density functional theory (DFT), which replaces the complicated many-body electron interactions with quasi particles interacting via an exchange and correlation functional. Exchange and correlation functionals based on the local density approximation (LDA), general gradient approximation (GGA) and hybrid functionals predict formation energies in a range of 2 eV–4.5 eV [21]. Green's function based methods, such as the *GW* approximation, are expected to yield more accurate results and predict formation energies of about 4.5 eV [18]. A low-scaling implementation of the random-phase approximation reported formation energies on a similar scale [37]. Quantum Monte Carlo (QMC) provides another computationally more expensive alternative to DFT and is among the most accurate electronic structure methods available. Several groups have calculated the formation energies using quantum Monte Carlo (QMC) [36, 38]. In this work, we focus only on the former [36], because it employs a

Slater-Jastrow-backflow wavefunction, which changes the formation energies substantially.

The CC method is a systematically improvable many-electron theory, which is widely used in molecular quantum chemistry, where it achieves high accuracy in the prediction of reaction energies for a wide range of systems. While being an efficient method for calculating small to medium-sized molecules, single-reference CC methods have never been used to calculate the formation energies of silicon self-interstitials and the vacancy in diamond cubic crystal silicon. Only over the past few years have computationally efficient implementations of periodic CC methods become available to study such systems [39–42]. Moreover, recent developments in embedding approaches also make it possible to study such local phenomena using CC methods [43–51]. The goal of this work is to calculate the formation energies of the silicon self-interstitials and vacancy at the level of coupled cluster singles doubles and perturbative triples (CCSD(T)) theory and compare them to experimental data [35, 52–55] and reference data from literature [18, 21, 36, 37].

## II. THEORY AND METHODS

### A. Hartree-Fock (HF) and CC theory

In HF theory, the many-body wavefunction is approximated by a single Slater determinant, and the energy is optimized with respect to variations of the spin orbitals used to construct the Slater determinant. The Slater determinant constructed from these spin orbitals is the HF ground state wavefunction  $|0\rangle$  and can be interpreted as a new vacuum from which particle-hole pair excitations are created and annihilated in the context of quantum field theory. Building on one-body theories such as HF, CC theory employs an exponential ansatz acting on a single Slater determinant.

$$|\Psi_{CC}\rangle = e^{\hat{T}} |0\rangle, \quad (1)$$

$$\hat{T} = \sum_{i,a} t_i^a \hat{a}_a^\dagger \hat{a}_i + \frac{1}{4} \sum_{i,j,a,b} t_{ij}^{ab} \hat{a}_a^\dagger \hat{a}_b^\dagger \hat{a}_j \hat{a}_i + \dots \quad (2)$$

Herein, the indices  $i, j$  and  $a, b$  refer to particle (unoccupied) and hole (occupied) states, respectively. By projecting onto the excited Slater determinants, one obtains a set of coupled non-linear equations, that can be solved for the amplitudes  $t_i^a, t_{ij}^{ab}$ , etc. using iterative methods. For practical calculations, the cluster operator  $\hat{T}$  has to be truncated, usually to single and double excitations. While including the full triple excitation manifold is computationally too expensive, an estimate of the connected triples contribution can be calculated noniteratively using an expression reminiscent of many-body perturbation theory. This method is referred to as CCSD(T) theory [56]. A more detailed description of CC methods can be found in Ref. [57, 58].

### B. Basis set and finite size error correction

All practical post-Hartree-Fock calculations of real materials employ a finite number of particle states also referred to as virtual orbitals  $N_v$ . The truncation of the virtual orbital basis set introduces the basis set incompleteness error (BSIE). The BSIE vanishes very slowly in the limit of  $N_v \rightarrow \infty$ . This observation is not surprising since the leading order basis set error originates from the so-called electron-electron cusp conditions [59], which are in real space a short-ranged electronic correlation phenomenon. Explicitly correlated methods help reduce the finite basis set error substantially [60, 61]. These methods, as well as their application to periodic systems, have already been discussed extensively elsewhere [62–64]. In order to treat the BSIE we use a pair-specific cusp correction for CC theory [65]. This scheme is based on frozen natural orbitals (FNOs) and diagrammatically decomposed contributions to the electronic correlation energy, which dominates the BSIE. To partly account for the BSIE of the (T) contribution to the CCSD(T) correlation energy, we rescale the (T) contribution using the ratio of the CCSD correlation energy with and without the BSIE correction discussed above.

Further, we simulate the silicon crystal using a periodic supercell approach with a finite system size. The employed finite system introduces the finite size error (FSIE). It should be noted that many properties, including the ground state energy, converge slowly with respect to the system size. This originates from the fact that correlated wavefunction-based theories capture longer ranged electronic correlation effects such as dispersion interaction explicitly. The coupled cluster correlation energy can be expressed as an integral over the electronic transition structure factor multiplied by the Coulomb kernel in reciprocal space. Finite size errors partly originate from an incomplete sampling of this integral in reciprocal space. Here, we employ an interpolation technique that can be used to evaluate the correlation energy integral more accurately, reducing the finite size error. The technical details are described in reference [66].

### C. Cell structure

The employed simulation cells of silicon self-interstitials are obtained by adding one Si atom to the diamond cubic crystal structure of bulk silicon and relaxing the atomic positions. The energetically most stable silicon self-interstitial (X) is one in which two silicon atoms reside symmetrically shifted from the position previously occupied by one. The two atoms are oriented parallel to the [110] direction. The second most favorable self-interstitial (H) is where the additional Si atom is equidistant to six other atoms, forming a hexagonal ring. It is worth noting that this configuration is unstable in DFT-PBE, where the central atom of the ring is

slightly moving away in a direction orthogonal to the ring (C3V) [18, 67]. The last self-interstitial considered in this work, with the highest energy, is where the additional Si atom is coordinated equidistantly to four nearest neighbors, forming a tetrahedron (T). For the T interstitial, the highest occupied state is threefold degenerate but only occupied by two electrons, which potentially introduces a multireference character. The vacancy is created by removing one Si atom from the bulk structure. Like the T interstitial, it has a threefold degenerate highest occupied state, occupied by two electrons. The vacancy is known to undergo a Jahn-Teller distortion to a  $D_{2d}$  symmetry [68].

All the ion positions of the used structures have been relaxed at the DFT level using the PBE exchange and correlation energy functional [69]. The shape and volume of the cells are kept fixed during the relaxation procedure.

#### D. Computational Details

All coupled-cluster calculations have been performed using our high-performance open-source coupled cluster simulation code, coupled cluster for solids (C`c4s`). The preparation of the necessary reference wavefunction and the required intermediates was performed using the Vienna ab initio simulation package (VASP) [70–72]. For all calculations in VASP a plane-wave kinetic energy cut off of  $E_{\text{cut}} = 400$  eV has been used. The employed smearing parameter is  $\sigma = 10^{-4}$  eV and a convergence criterion of  $\Delta E = 10^{-6}$  eV is used. All other numerical parameters were left unchanged from their default values. The HF calculations are performed using VASP and the structures described in section II C. The HF calculations are done using a  $\Gamma$ -centered  $7 \times 7 \times 7$   $k$ -point mesh. All post-HF calculations sample the first Brillouin zone using a single  $k$ -point only. Further, we need to compute all unoccupied HF orbitals since in CC theory we approximate the many-electron wavefunction using excited Slater determinants, constructed by occupied and unoccupied HF orbitals. In VASP this is achieved by setting the number of virtual orbitals to the maximum number of plane-waves in the basis set. The convergence of the coupled cluster singles doubles (CCSD) electron correlation energy is very slow when using canonical HF orbitals. A much faster convergence to the complete basis set limit is achieved using natural orbitals. In VASP approximate natural orbitals can be calculated as described in Eq.(2) from Ref. [73]. After calculating all natural orbitals, a subset of them is chosen for the C`c4s` calculations. For the coupled-cluster theory calculations, we chose the number of unoccupied natural orbitals per occupied orbital to be 5, 10, 15, 20, 25 and 30. Additionally, for the basis set correction algorithm described in section II B and in the references therein, the second-order Møller-Plesset perturbation theory (MP2) pair energies are needed. For this purpose, there are two algorithms available in VASP [74, 75]. In our case, we have used a

16-atom cell for the bulk with 32 occupied orbitals; therefore, the MP2 algorithm from Ref. [75] is more efficient. In the case of more than 50 occupied orbitals, a different algorithm based on Laplace transformed MP2 (LTMP2) might be faster and less memory consuming [74]. Note that the basis set correction algorithm uses a focal-point approach, and from now on, the basis set correction is also referred to as the focal-point correction (FPC). With these preparations done, VASP can provide all necessary files needed for the CCSD(T) calculation with the finite size and basis set error correction computed by C`c4s`. It is worth noting that the CCSD calculation in C`c4s` converges much faster when using the direct inversion of the iterative subspace (DIIS) mixer instead of the default linear mixer. The described workflow with all necessary files can be found on GitHub or zenodo [76, 77].

After studying the BSIE, we chose our number of virtual orbitals per occupied orbital to be 10 and repeated all calculations with 10 randomly chosen  $k$ -point shifts in order to get a twist average estimate of the CCSD(T) correlation energies.

All calculations have been performed using 16 compute nodes, each equipped with 384 GB main memory.

### III. RESULTS

We now discuss the formation energies of the silicon self-interstitial structures described in section II C at the CCSD(T) level of theory. We use 16 atom cells for the pristine bulk crystal with periodic boundary conditions, the interstitial cells have 17 atoms, while the vacancy has 15 atoms. The HF energies, CCSD, CCSD(T), finite size and basis set energy corrections can be found in the supplementary material, in table I. The formation energy is calculated by subtracting the energy of the interstitial cell with the energy of the bulk cell scaled to the same number of atoms:

$$E_{\text{F}} = E_{\text{int}} - \frac{N_{\text{int}}}{N_{\text{bulk}}} E_{\text{bulk}}. \quad (3)$$

We first discuss the convergence of the HF energy contribution to the formation energies. Figure 1 shows the convergence of the HF formation energies with respect to the size of the  $k$ -point mesh used in the HF calculation. We used a  $\Gamma$ -centered cubic  $k$ -point mesh with up to  $7 \times 7 \times 7$  grid points. Using only one  $k$ -point gives qualitatively and quantitatively wrong formation energies. With a  $k$ -point mesh size of  $5 \times 5 \times 5$ , the formation energies are already well converged and increasing the  $k$ -point grid size further to  $7 \times 7 \times 7$  increases the formation energies of X, H and C3V by less than 8.5 meV, while T and V increase by 29 meV and 19 meV. We now discuss the convergence of the correlation energy contributions to the formation energies with respect to the number of virtual orbitals. Let us note that the HF formation energy Contributions are independent of the virtual orbital basis set size. The MP2 calculations employ the complete virtual

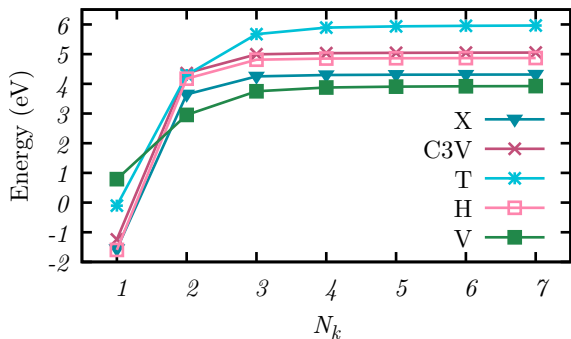


FIG. 1. The formation energy as a function of the number of  $k$ -points used in the Hartree-Fock calculation for all self-interstitials. A  $\Gamma$ -centered cubic  $k$ -point mesh was used with  $N_k \times N_k \times N_k$  gridpoints.

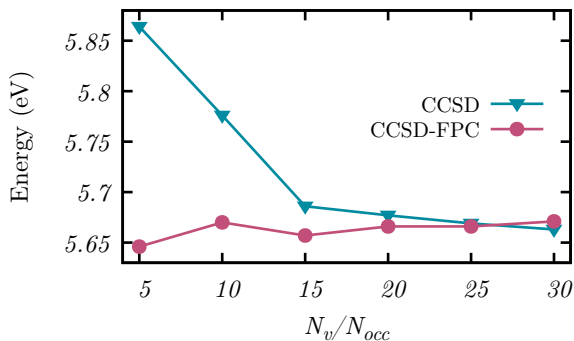


FIG. 2. CCSD formation energy of the X interstitial as a function of the number of orbitals per occupied orbital with and without the basis set correction scheme (FPC). A  $\Gamma$ -centered cubic mesh was used.

orbital basis set defined by the kinetic energy cutoff of the plane wave basis set. Furthermore the MP2 correlation energies are automatically extrapolated to the complete basis set limit using a procedure explained in Ref. [74]. For the post-MP2 correlation energy calculations, we employ approximate natural orbitals as virtual orbitals and seek to converge the correlation energies explicitly by increasing the number of virtual orbitals. We find that this approach allows for an effective cancellation between basis set incompleteness errors of correlation energies for different systems when taking their differences. Furthermore, we add a basis set incompleteness error correction described in Ref. [65] to accelerate the convergence of the CCSD correlation energy. The effect of the basis set correction on the formation energy is highlighted in figure 2, which depicts the formation energy retrieved as a function of the number of virtual orbitals per occupied orbital for the X interstitial. Our results indicate that between 10 and 20 virtual orbitals per occupied orbital suffice to achieve converged formation energies with and without the basis set correction, respectively. The remaining

basis set incompleteness error is caused by fluctuations on the scale of about 10 meV, which is smaller than the expected accuracy of the employed theories. Figure 3

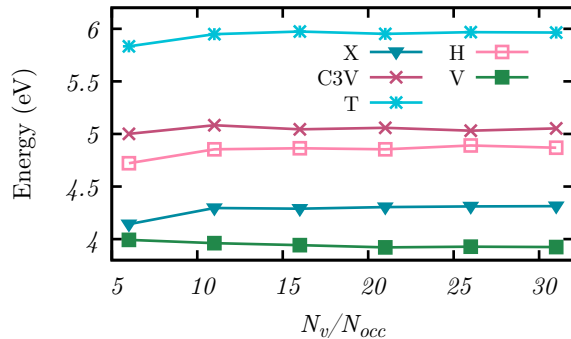


FIG. 3. CCSD(T) formation energies as a function of the number of virtual orbitals per occupied orbital for all self-interstitials include finite size and basis set corrections.

shows the convergence of the CCSD(T) formation energies of all self-interstitials with respect to the number of natural orbitals, including the finite size and basis set corrections. Note that the basis set correction behaves similarly for all self-interstitials. From figure 3, we see that  $N_v/N_{occ} = 10$  is already accurate enough to assume convergence within chemical accuracy ( $\approx 43$  meV).

With  $N_v/N_{occ} = 10$ , we repeat all calculations at 10 random  $k$ -points in order to obtain a twist-averaged estimate of the correlation energy contribution to the formation energies. This approach reduces finite size errors in CC calculations that originate from single-particle effects [41]. The energy corrections for the twist averaging can be found in the supplementary material, in tables II-VII. Using 10 random  $k$ -points our standard deviation from the average CCSD(T) energy is in decreasing order for  $E_F(T) = 227$  meV,  $E_F(V) = 101$  meV,  $E_F(X) = 80$  meV,  $E_F(C3V) = 73$  meV and  $E_F(H) = 51$  meV. After twist averaging, the formation energy of V, T and X increases by 818 meV, 367 meV and 239 meV. While the formation energy of the C3V and H interstitial decreases by 85 meV and 44 meV, indicating that it is important to account for this contribution.

For completeness, we summarize the obtained formation energies at the different levels of theory again in table I. The HF energies, CCSD, CCSD(T), finite size and basis set energy corrections can be found in the supplementary material, in table I.

Next, we briefly discuss the effect of the FSIE correction based on the structure factor interpolation, which accounts for two-electron finite size errors. Table I summarizes the computed CCSD formation energies with and without the corresponding finite size correction denoted as CCSD-FS and CCSD, respectively. It is not surprising that this correction is significant and on the scale of about 0.5 eV. However, based on previous results re-

TABLE I. CCSD and CCSD(T) formation energies of the silicon self-interstitials and the vacancy with and without the basis set and finite size correction as a function of the unoccupied to occupied orbital ratio  $N_v/N_{occ}$  at the  $\Gamma$ -point. FPC and FS denote that the basis set/finite size corrections are included.

HF/MP2	$N_v/N_{occ}$	CCSD	CCSD(T)	CCSD-FS	CCSD-FPC	CCSD-FS-FPC	CCSD(T)-FS-FPC
C3V	5	6.659	5.981	6.149	6.334	5.824	5.001
8.502	10	6.484	5.753	6.012	6.343	5.871	5.083
4.408	15	6.374	5.614	5.907	6.305	5.837	5.044
	20	6.347	5.577	5.880	6.317	5.850	5.059
	25	6.330	5.556	5.864	6.288	5.822	5.031
	30	6.315	5.537	5.849	6.308	5.843	5.053
X	5	5.864	5.094	5.285	5.646	5.067	4.142
7.930	10	5.776	4.982	5.254	5.670	5.148	4.296
3.780	15	5.686	4.866	5.169	5.657	5.141	4.289
	20	5.677	4.853	5.162	5.666	5.150	4.305
	25	5.669	4.842	5.155	5.666	5.152	4.311
	30	5.663	4.831	5.150	5.671	5.158	4.313
T	5	7.857	7.051	7.238	7.435	6.816	5.833
9.954	10	7.628	6.764	7.055	7.455	6.882	5.949
5.355	15	7.531	6.641	6.964	7.469	6.902	5.974
	20	7.511	6.611	6.944	7.447	6.880	5.952
	25	7.489	6.584	6.923	7.458	6.892	5.968
	30	7.476	6.565	6.910	7.456	6.890	5.964
H	5	6.358	5.717	5.877	5.986	5.504	4.722
8.162	10	6.231	5.538	5.783	6.053	5.605	4.854
4.212	15	6.132	5.413	5.689	6.058	5.615	4.864
	20	6.103	5.376	5.661	6.046	5.604	4.854
	25	6.090	5.360	5.649	6.075	5.635	4.890
	30	6.075	5.341	5.634	6.056	5.616	4.869
V	5	5.291	4.866	4.820	4.999	4.528	3.993
5.554	10	5.034	4.546	4.573	4.952	4.492	3.961
4.305	15	4.960	4.443	4.500	4.942	4.483	3.942
	20	4.942	4.413	4.484	4.925	4.467	3.921
	25	4.926	4.394	4.470	4.928	4.472	3.928
	30	4.919	4.380	4.462	4.928	4.472	3.924

ported in Ref. [41] we expect that the employed finite size correction will suffice for the 16/17 atom cells to achieve chemical accuracy in the convergence of the computed formation energies with respect to the employed system size. Furthermore, it can be concluded from the comparison between CCSD-FS and CCSD in table I, that the computed finite size correction is already well converged using  $N_v/N_{occ} = 10$ . Note that the finite size correction can currently only be applied to the CCSD calculation. The (T) contribution to the formation energies is significantly smaller than the CCSD correlation energy contribution, which makes it plausible to neglect the finite size correction to the (T) contribution.

Table I also includes results for the vacancy formation energy. We note that these calculations employ a 15-atom cell only. Due to the small supercell size, the system does not undergo a Jahn-Teller distortion [68], which can be observed for larger cells and which significantly changes the formation energy. Therefore, we note that these results are only meaningful as benchmarks for other theories employing identical geometries and can not be

compared to experiment. Our best estimates of the formation energies at the level of HF, CCSD and CCSD(T) theory including all corrections discussed above are compared to values from the literature and experiment in table II. We see that the formation energies calculated with LDA and PBE are small (3–4 eV) and close to each other for all self-interstitials, with a difference of 80 – 160 meV. Yet the order of stability is not the same; for LDA the most stable self-interstitial is X then H and T. For PBE T has a lower energy than H. Incorporating a portion of the exact exchange correlation energy in the HSE functional increases the formation energies, and their difference to 360 meV and 100 meV, with the order of stability of X, H and T. RPA predicts the same order of stability with a difference between X and H of 180 meV, while the difference between H and T is 80 meV. Increasing the cell size to 216 atoms changes the differences significantly to 130 meV and 600 meV, still with the same order of stability.  $G_0W_0$  for 16 atom cells predicts that H is more stable than X while their difference is only 60 meV. In QMC, using 16 atom cells without a backflow correction,

TABLE II. Computed and converged HF, CCSD and CCSD(T) formation energies including all reported corrections in this work compared to QMC [36], RPA [37], PBE [37], LDA [18, 21],  $G_0W_0$  [18] and HSE [21] from the literature and also experimental data [35, 52–55]. All results have been obtained for the 16/17 atom cells except RPA(216), which employed 216/217 atom cells.

Cell	HF	CCSD	CCSD(T)	QMC	QMC (nobf)	$G_0W_0$	RPA	RPA (216)	HSE	PBE	LDA	Exp.
X	7.930	5.295	4.535	4.4	4.9	4.46	4.27	4.2	4.46	3.56	3.29	
T	9.954	7.127	6.316	5.1	5.2		4.53	4.93	4.92	3.66	3.56	
H	8.162	5.559	4.810	4.7	4.9	4.4	4.45	4.33	4.82	3.74	3.4	4.2 – 4.7

X and H are nearly degenerate, while the difference to T is 300 meV. Including the backflow correction gives the order of stability as X, H and T with clear differences of 300 meV and 400 meV. We now turn to the wavefunction methods employed in this work. The formation energies calculated with HF are much larger than the ones calculated with the other theories presented. While the order of stability is in agreement with the corrected QMC calculations, their difference is 232 meV and 1792 meV. Expanding the correlation space further to CCSD and CCSD(T) theory, including the basis set and finite size correction, lowers the formation energies by 2.8–2.6 eV and another 811–749 meV. Their relative difference also changes to 264 meV and 1568 meV for CCSD theory and 275 meV and 1506 meV for CCSD(T) theory. Our estimated CCSD(T) formation energies are in good agreement with extrapolated QMC calculations [36] employing a Slater-Jastrow-backflow correction for the X and H interstitial. However, we have a discrepancy of 1.2 eV for the T interstitial. This could stem from the fact that in DFT the energetically highest occupied orbitals are threefold degenerate while being occupied by two electrons. It may be an indication that a multireference treatment is needed. Our CCSD(T) formation energy for the H interstitial is within reasonable agreement with experiment, being 110 meV above the experimental upper bound.

#### IV. CONCLUSION AND SUMMARY

In this paper, we have calculated the formation energies of the silicon self-interstitials and the vacancy in a periodic supercell at the CCSD(T) level of theory. We have used correction schemes tailored to CC theory to reduce the BSIE and the FSIE. Our results have been compared to data from the literature and experiment, including LDA, PBE, HSE, RPA,  $G_0W_0$  and QMC.

In general, DFT using the LDA and PBE functionals fails to differentiate the structures, resulting in small energy differences between the self-interstitials while also underestimating the formation energies. Additionally, HF overestimates the formation energies. The HSE functional offers a compromise, and its formation energies are in good agreement with the much more expensive and accurate QMC calculations. The QMC formation energies

of the two most stable self-interstitials, X and H, are nearly degenerate. This degeneracy is lifted by employing the Slater-Jastrow-backflow trial wavefunction [36].

Our CCSD(T) formation energies are in good agreement with QMC calculations employing a Slater-Jastrow-backflow wavefunction for the X and H interstitials. The CCSD(T) formation energy for the H interstitial is within reasonable agreement with experimental data, being 110 meV above the upper bound. However, the CCSD(T) formation energy of the T interstitial is 1.2 eV higher than in the QMC calculations. Since in DFT the highest occupied orbital of the T interstitial is threefold degenerate but only occupied by two electrons, we suppose a multireference approach may be necessary. We stress that none of the discussed methods is expected to work for strongly correlated systems. DFT based approaches underestimate the formation energy of strongly correlated defects due to the introduction of partly filled orbitals that reduce the self-interaction error. QMC techniques require multideterminant trial wavefunctions for strongly correlated systems to reduce the error from the fixed-node approximations, and RPA is expected to inherit part of the DFT errors for the treatment of strongly correlated systems. Therefore, we have to conclude that more sophisticated theories will be needed in future studies to fully resolve the observed discrepancy for the formation energy of the T interstitial.

Although we demonstrated that basis set convergence can be achieved efficiently at the level of CCSD(T) theory using recently presented methods, the treatment of finite size errors is still challenging and relatively large defect concentrations had to be employed. However, we note that recently developed embedding methods will allow to investigate much lower defect concentrations in a computationally efficient manner [78].

#### ACKNOWLEDGEMENTS

The authors thankfully acknowledge support and funding from the European Research Council (ERC) under the European Union’s Horizon 2020 research and innovation program (Grant Agreement No 715594). The computational results presented have been achieved using the Vienna Scientific Cluster (VSC).

- 
- [1] K. Graff, *Metal impurities in silicon-device fabrication*, Vol. 24 (Springer Science & Business Media, 2013).
- [2] E. Weber, *Kristall und Technik* **16**, 209 (1981).
- [3] G. Watkins and S. Pantelides, Gordon Breach, New York (1986).
- [4] G. D. Watkins, *Materials Science in Semiconductor Processing* **3**, 227 (2000).
- [5] O. Breitenstein and J. Heydenreich, *Scanning* **7**, 273 (1985).
- [6] N. Fukata and M. Suezawa, *Journal of Applied Physics* **86**, 1848 (1999).
- [7] R. J. Tilley, in *Encyclopedia of Inorganic and Bioinorganic Chemistry* (John Wiley and Sons, Ltd, 2018) pp. 1–23.
- [8] P. M. Fahey, P. B. Griffin, and J. D. Plummer, *Rev. Mod. Phys.* **61**, 289 (1989).
- [9] D. J. Eaglesham, P. A. Stolk, H. Gossmann, and J. M. Poate, *Applied Physics Letters* **65**, 2305 (1994).
- [10] D. A. Richie, J. Kim, S. A. Barr, K. R. A. Hazzard, R. Hennig, and J. W. Wilkins, *Phys. Rev. Lett.* **92**, 045501 (2004).
- [11] R. Vaidyanathan, M. Y. L. Jung, and E. G. Seebauer, *PHYSICAL REVIEW B* **75** (2007), 10.1103/PhysRevB.75.195209.
- [12] D. Riedel, F. Fuchs, H. Kraus, S. Väh, A. Sperlich, V. Dyakonov, A. A. Soltamova, P. G. Baranov, V. A. Ilyin, and G. V. Astakhov, *Phys. Rev. Lett.* **109**, 226402 (2012).
- [13] A. M. Tyryshkin, S. Tojo, J. J. L. Morton, H. Riemann, N. V. Abrosimov, P. Becker, H.-J. Pohl, T. Schenkel, M. L. W. Thewalt, K. M. Itoh, and S. A. Lyon, *Nature Materials* **11**, 143 (2011).
- [14] K. Otsuka and X. Ren, *Intermetallics* **7**, 511 (1999).
- [15] W. Gao and A. Tkatchenko, *Phys. Rev. Lett.* **111**, 045501 (2013).
- [16] F. Bruneval, *Phys. Rev. Lett.* **108**, 256403 (2012).
- [17] R. Ramprasad, H. Zhu, P. Rinke, and M. Scheffler, *Phys. Rev. Lett.* **108**, 066404 (2012).
- [18] P. Rinke, A. Janotti, M. Scheffler, and C. G. Van de Walle, *Phys. Rev. Lett.* **102**, 026402 (2009).
- [19] C. G. Van de Walle and A. Janotti, *physica status solidi (b)* **248**, 19 (2011).
- [20] C. G. Van de Walle and J. Neugebauer, *Journal of Applied Physics* **95**, 3851 (2004).
- [21] E. R. Batista, J. Heyd, R. G. Hennig, B. P. Uberuaga, R. L. Martin, G. E. Scuseria, C. J. Umrigar, and J. W. Wilkins, *Phys. Rev. B* **74**, 121102 (2006).
- [22] W.-K. Leung, R. J. Needs, G. Rajagopal, S. Itoh, and S. Ihara, *Phys. Rev. Lett.* **83**, 2351 (1999).
- [23] P. E. Blöchl, E. Smargiassi, R. Car, D. B. Laks, W. Andreoni, and S. T. Pantelides, *Phys. Rev. Lett.* **70**, 2435 (1993).
- [24] Y. Bar-Yam and J. D. Joannopoulos, *Phys. Rev. B* **30**, 1844 (1984).
- [25] R. Vaidyanathan, M. Y. L. Jung, and E. G. Seebauer, *Phys. Rev. B* **75**, 195209 (2007).
- [26] V. Ranki and K. Saarinen, *Phys. Rev. Lett.* **93**, 255502 (2004).
- [27] H. Bracht, J. F. Pedersen, N. Zangenberg, A. N. Larsen, E. E. Haller, G. Lulli, and M. Posselt, *Phys. Rev. Lett.* **91**, 245502 (2003).
- [28] A. Ural, P. B. Griffin, and J. D. Plummer, *Phys. Rev. Lett.* **83**, 3454 (1999).
- [29] H. Bracht, E. E. Haller, and R. Clark-Phelps, *Phys. Rev. Lett.* **81**, 393 (1998).
- [30] H. Bracht, N. A. Stolwijk, and H. Mehrer, *Phys. Rev. B* **52**, 16542 (1995).
- [31] H. Bracht, H. H. Silvestri, I. D. Sharp, and E. E. Haller, *Phys. Rev. B* **75**, 035211 (2007).
- [32] Y. Shimizu, M. Uematsu, and K. M. Itoh, *Phys. Rev. Lett.* **98**, 095901 (2007).
- [33] P. M. Fahey, P. B. Griffin, and J. D. Plummer, *Rev. Mod. Phys.* **61**, 289 (1989).
- [34] S. Dannefaer, P. Mascher, and D. Kerr, *Phys. Rev. Lett.* **56**, 2195 (1986).
- [35] A. Ural, P. B. Griffin, and J. D. Plummer, *Journal of Applied Physics* **85**, 6440 (1999).
- [36] W. D. Parker, J. W. Wilkins, and R. G. Hennig, *physica status solidi (b)* **248**, 267 (2011).
- [37] M. Kaltak, J. c. v. Klimeš, and G. Kresse, *Phys. Rev. B* **90**, 054115 (2014).
- [38] W. K. Leung, R. Needs, G. Rajagopal, S. Itoh, and S. Ihara, *VLSI Design* **13** (2001), 10.1155/2001/83797.
- [39] G. H. Booth, A. Grüneis, G. Kresse, and A. Alavi, *Nature* **493**, 365 (2013).
- [40] T. Gruber and A. Grüneis, *Phys. Rev. B* **98**, 134108 (2018).
- [41] T. Gruber, K. Liao, T. Tsatsoulis, F. Hummel, and A. Grüneis, *Phys. Rev. X* **8**, 021043 (2018).
- [42] J. McClain, Q. Sun, G. K.-L. Chan, and T. C. Berkelbach, *J. Chem. Theory Comput.* **13**, 1209 (2017), pMID: 28218843.
- [43] M. Schütz, L. Maschio, A. J. Karttunen, and D. Usvyat, *The Journal of Physical Chemistry Letters* **8**, 1290 (2017).
- [44] D. Usvyat, L. Maschio, and M. Schütz, *WIREs Computational Molecular Science* **8**, 1 (2018).
- [45] M. Nusspickel and G. H. Booth, *Phys. Rev. X* **12**, 011046 (2022).
- [46] J. Chen, N. A. Bogdanov, D. Usvyat, W. Fang, A. Michaelides, and A. Alavi, *The Journal of Chemical Physics* **153**, 204704 (2020).
- [47] J. Sauer, *Accounts of Chemical Research* **52**, 3502 (2019).
- [48] H. H. Lin, L. Maschio, D. Kats, D. Usvyat, and T. Heine, *Journal of Chemical Theory and Computation* **16**, 7100 (2020).
- [49] J. D. Goodpaster, T. A. Barnes, F. R. Manby, and T. F. Miller, *The Journal of Chemical Physics* **140**, 18A507 (2014).
- [50] T. Schäfer, F. Libisch, G. Kresse, and A. Grüneis, *The Journal of Chemical Physics* **154**, 011101 (2021).
- [51] B. T. G. Lau, G. Knizia, and T. C. Berkelbach, *The Journal of Physical Chemistry Letters* **12**, 1104 (2021), pMID: 33475362.
- [52] P. M. Fahey, P. B. Griffin, and J. D. Plummer, *Rev. Mod. Phys.* **61**, 289 (1989).
- [53] H. Bracht, N. A. Stolwijk, and H. Mehrer, *Phys. Rev. B* **52**, 16542 (1995).
- [54] H. Bracht, E. E. Haller, and R. Clark-Phelps, *Phys. Rev. Lett.* **81**, 393 (1998).
- [55] A. Ural, P. B. Griffin, and J. D. Plummer, *Phys. Rev. Lett.* **83**, 3454 (1999).

- [56] K. Raghavachari, G. W. Trucks, J. A. Pople, and M. Head-Gordon, *Chemical Physics Letters* **157**, 479 (1989).
- [57] R. J. Bartlett and M. Musiał, *Rev. Mod. Phys.* **79**, 291 (2007).
- [58] R. J. B. Isaiah Shavitt, 1st ed., *Cambridge Molecular Science* (Cambridge University Press, 2009).
- [59] T. Kato, *Communications on Pure and Applied Mathematics* **10**, 151 (1957).
- [60] C. Hättig, W. Klopper, A. Köhn, and D. P. Tew, *Chemical Reviews* **112**, 4 (2012), pMID: 22206503.
- [61] S. Ten-no, *Theoretical Chemistry Accounts* **131**, 1070 (2012).
- [62] A. Grüneis, *Phys. Rev. Lett.* **115**, 066402 (2015).
- [63] A. Grüneis, J. J. Shepherd, A. Alavi, D. P. Tew, and G. H. Booth, *The Journal of Chemical Physics* **139**, 084112 (2013).
- [64] D. Usvyat, *The Journal of Chemical Physics* **139**, 194101 (2013).
- [65] A. Irmeler, A. Gallo, and A. Grüneis, *The Journal of Chemical Physics* **154**, 234103 (2021).
- [66] K. Liao and A. Grüneis, *The Journal of Chemical Physics* **145**, 141102 (2016).
- [67] O. K. Al-Mushadani and R. J. Needs, *Phys. Rev. B* **68**, 235205 (2003).
- [68] F. Corsetti and A. A. Mostofi, *Phys. Rev. B* **84**, 035209 (2011).
- [69] J. P. Perdew, K. Burke, and M. Ernzerhof, *Phys. Rev. Lett.* **77**, 3865 (1996).
- [70] G. Kresse and J. Hafner, *Phys. Rev. B* **47**, 558 (1993).
- [71] G. Kresse and J. Furthmüller, *Phys. Rev. B* **54**, 11169 (1996).
- [72] G. Kresse and J. Furthmüller, *Computational Materials Science* **6**, 15 (1996).
- [73] A. Grüneis, G. H. Booth, M. Marsman, J. Spencer, A. Alavi, and G. Kresse, *Journal of Chemical Theory and Computation* **7**, 2780 (2011), pMID: 26605469.
- [74] T. Schäfer, B. Ramberger, and G. Kresse, *The Journal of Chemical Physics* **146**, 104101 (2017).
- [75] M. Marsman, A. Grüneis, J. Paier, and G. Kresse, *The Journal of Chemical Physics* **130** (2009), 10.1063/1.3126249, 184103.
- [76] F. Salihbegovic, “Silicon interstitials ccsd(t),” (2023).
- [77] Salihbegovic, “salihbegovic/silicon-ccsd-t: Workflow si-interstitials ccsd(t),” (2023).
- [78] T. Schäfer, F. Libisch, G. Kresse, and A. Grüneis, *The Journal of Chemical Physics* **154**, 011101 (2021).



# Supporting information: Formation energies of silicon self-interstitials using periodic coupled cluster theory

Faruk Salihbegović, Alejandro Gallo, and Andreas Grüneis

*Institute for Theoretical Physics, Vienna University of Technology (TU Wien). A-1040 Vienna, Austria, EU.*

arXiv:2306.11669v2 [cond-mat.mtrl-sci] 22 Jun 2023

## I. $\Gamma$ -POINT CALCULATIONS AND BASIS SET CONVERGENCE

Table I shows the coupled cluster singles doubles (CCSD) and coupled cluster singles doubles and perturbative triples (CCSD(T)) energy corrections to the Hartree-Fock (HF) ground state energies, as well as the basis set and the finite size correction. The HF energy was calculated using a  $\Gamma$ -centered  $7 \times 7 \times 7$   $k$ -point mesh. All the other corrections were calculated at the  $\Gamma$ -point.

TABLE I. HF formation energies of all calculated structures, as well as the CCSD, CCSD(T), finite size and basis set corrections. All energies are in eV.

HF	$N_v/N_{occ}$	CCSD	CCSD(T)	FS	BS
Bulk -151.920	5	-43.4765	-2.3715	-3.7478	-9.7135
	10	-49.9044	-3.4427	-3.8412	-4.0339
	15	-51.6199	-3.7680	-3.8593	-2.4171
	20	-52.3780	-3.9174	-3.8633	-1.6891
	25	-52.8151	-4.0039	-3.8653	-1.2599
	30	-53.0515	-4.0461	-3.8654	-1.0200
C3V -152.9134	5	-48.0369	-3.1975	-4.4917	-10.6451
	10	-55.0409	-4.3890	-4.5530	-4.4268
	15	-56.9736	-4.7637	-4.5677	-2.6377
	20	-57.8062	-4.9321	-4.5715	-1.8250
	25	-58.2881	-5.0274	-4.5724	-1.3807
	30	-58.5542	-5.0770	-4.5723	-1.0903
X -153.4851	5	-48.2597	-3.2894	-4.5609	-10.5387
	10	-55.1774	-4.4519	-4.6033	-4.3915
	15	-57.0905	-4.8230	-4.6169	-2.5965
	20	-57.9043	-4.9867	-4.6201	-1.8062
	25	-58.3773	-5.0805	-4.6210	-1.3409
	30	-58.6339	-5.1316	-4.6207	-1.0757
T -151.4606	5	-48.2917	-3.3253	-4.6008	-10.7425
	10	-55.3498	-4.5223	-4.6540	-4.4593
	15	-57.2692	-4.8940	-4.6676	-2.6304
	20	-58.0948	-5.0627	-4.6716	-1.8590
	25	-58.5816	-5.1593	-4.6727	-1.3693
	30	-58.8459	-5.2094	-4.6727	-1.1039
H -153.2528	5	-47.9977	-3.1610	-4.4635	-10.6933
	10	-54.9550	-4.3508	-4.5291	-4.4641
	15	-56.8764	-4.7222	-4.5437	-2.6421
	20	-57.7108	-4.8892	-4.5467	-1.8522
	25	-58.1881	-4.9839	-4.5476	-1.3534
	30	-58.4548	-5.0331	-4.5472	-1.1027
V -136.8709	5	-41.0219	-2.6484	-3.9846	-9.3988
	10	-47.3057	-3.7151	-4.0613	-3.8637
	15	-48.9880	-4.0494	-4.0775	-2.2835
	20	-49.7164	-4.2020	-4.0798	-1.6001
	25	-50.1419	-4.2861	-4.0802	-1.1794
	30	-50.3710	-4.3320	-4.0803	-0.9470

## II. RANDOM $k$ -POINT CALCULATIONS

Tables II-VII show the CCSD and CCSD(T) energy corrections to the HF ground state energies, as well as the basis set and the finite size correction for 10 random  $k$ -points using 10 virtual orbitals per occupied orbital.

TABLE II. All energies are in eV.

HF	CCSD	CCSD(T)	FS	BS
Bulk	-49.8167	-3.7600	-4.2053	-4.0146
-151.920	-49.7882	-3.6116	-4.0349	-4.0027
	-49.7887	-3.6936	-4.1435	-4.0076
	-49.7851	-3.6124	-4.0151	-4.0076
	-49.7881	-3.6590	-4.1462	-4.0077
	-49.8101	-3.7460	-4.1749	-4.0190
	-49.7918	-3.6290	-4.0086	-4.0090
	-49.8083	-3.7545	-4.2244	-4.0303
	-49.8207	-3.7633	-4.1717	-4.0173
	-49.7976	-3.7073	-4.1158	-4.0102
Average	-49.7995	-3.6937	-4.1240	-4.0126

TABLE III. All energies are in eV.

HF	CCSD	CCSD(T)	FS	BS
C3V	-55.0793	-4.6865	-4.8126	-4.3949
-152.9134	-55.0242	-4.5504	-4.6772	-4.3986
	-55.1168	-4.6773	-4.8237	-4.3960
	-55.0566	-4.5760	-4.6621	-4.3849
	-55.0991	-4.6385	-4.8578	-4.3967
	-55.1570	-4.7165	-4.7976	-4.3899
	-55.0867	-4.6046	-4.6337	-4.3900
	-55.1814	-4.7321	-4.9133	-4.3893
	-55.1799	-4.7372	-4.7677	-4.3942
	-55.1135	-4.6757	-4.7427	-4.3928
Average	-55.1094	-4.65948	-4.76885	-4.39272

TABLE IV. All energies are in eV.

HF	CCSD	CCSD(T)	FS	BS
X	-55.0427	-4.6651	-4.8119	-4.3681
-153.4851	-55.1184	-4.5860	-4.7078	-4.3438
	-55.0224	-4.6324	-4.7803	-4.3883
	-55.0596	-4.5699	-4.6657	-4.3641
	-55.0501	-4.6117	-4.8226	-4.3873
	-55.0537	-4.6725	-4.8059	-4.3848
	-55.0422	-4.5854	-4.6454	-4.3788
	-55.0168	-4.6710	-4.9005	-4.4082
	-55.0689	-4.6791	-4.7565	-4.3684
	-55.0544	-4.6451	-4.7333	-4.3727
Average	-55.0530	-4.63182	-4.76299	-4.37646

TABLE V. All energies are in eV.

HF	CCSD	CCSD(T)	FS	BS
T	-55.2699	-4.7589	-4.8835	-4.3863
-151.4606	-55.2986	-4.6747	-4.7801	-4.3943
	-55.3547	-4.7756	-4.8900	-4.3931
	-55.2511	-4.6547	-4.7454	-4.4002
	-55.1553	-4.6366	-4.8288	-4.3856
	-55.2156	-4.7206	-4.8375	-4.3851
	-55.0346	-4.5578	-4.6527	-4.4022
	-55.0616	-4.6681	-4.8444	-4.4209
	-55.1094	-4.6811	-4.7886	-4.3854
	-55.1468	-4.6625	-4.7681	-4.3789
Average	-55.1897	-4.67906	-4.80191	-4.39320

TABLE VI. All energies are in eV.

HF	CCSD	CCSD(T)	FS	BS
H	-55.0364	-4.6706	-4.7986	-4.3909
-153.2528	-54.9589	-4.5200	-4.6609	-4.3890
	-55.0356	-4.6364	-4.7915	-4.3832
	-54.9648	-4.5345	-4.6405	-4.3797
	-55.0054	-4.5977	-4.8300	-4.3916
	-55.0608	-4.6697	-4.7742	-4.3860
	-54.9979	-4.5684	-4.6153	-4.3882
	-55.0974	-4.6879	-4.8865	-4.3808
	-55.0909	-4.6923	-4.7437	-4.3858
	-55.0385	-4.6379	-4.7173	-4.3803
Average	-55.0287	-4.62153	-4.74585	-4.38555

TABLE VII. All energies are in eV.

HF	CCSD	CCSD(T)	FS	BS
V	-46.8932	-3.7864	-4.1677	-3.8147
-136.8709	-46.9264	-3.7007	-4.0489	-3.8173
	-46.9694	-3.7560	-4.1327	-3.7825
	-46.8965	-3.6820	-4.0553	-3.8076
	-46.8375	-3.6923	-4.0976	-3.8153
	-46.8939	-3.7783	-4.1499	-3.8024
	-46.8376	-3.6612	-4.0657	-3.8129
	-46.7661	-3.7462	-4.1541	-3.8628
	-46.8131	-3.7611	-4.1651	-3.8299
	-46.8483	-3.7296	-4.1263	-3.8017
Average	-46.8682	-3.72940	-4.11633	-3.81470